10B.3 THE USE OF RADIOSONDE-COSMIC COLLOCATION DATA TO IDENTIFY RADIOSONDE TYPE CHARACTERISTICS AND QUANTIFY IMPACTS OF COLLOCATION MISMATCH ON SATELLITE VALIDATION

Bomin Sun *
I. M. Systems Group, Rockville, Maryland

Anthony Reale
NOAA/NESDIS/STAR, Suitland, Maryland

Doug C. Hunt
UCAR COSMIC Office, Boulder, Colorado

1. INTRODUCTION

Historically global radiosonde observations (RAOBs) have been a key *dataset* in operational weather forecasting and upper-air climate trend detection. Due to their relatively high accuracy, radiosonde measurements have also been used as the "ground-truth" to calibrate and validate satellite sounding retrievals. Issues, however, exist in this application. Two of them, which are considered to have a great impact on the accuracy of satellite sounding calibration and validation, are described in the following paragraphs. By revealing these issues and providing possible solutions to them, the ultimate goal of the work is to improve the methodology of satellite sounding validation in weather monitoring.

RAOBs and satellite soundings are not perfectly collocated when the former are used to validate the latter. For most of the RAOB and polar satellite sounding collocations, the distance mismatch is in the range of 10 km to 90 km, and the time mismatch is in the range of 20 min to 6 hr. Collocation mismatches introduce weather noise into the validation which may lower the "accuracy" or "performance" of satellite soundings when they are evaluated by RAOBs in weather monitoring. This issue is compounded by the fact that radiosonde balloons drift with height. Balloons can take ~3 hr to ascend from surface to stratosphere and during this period they can drift over 200 km horizontally. One of the purposes of this study is to quantify the impact of collocation mismatch on sounding validation accuracy, and based on that, to provide guidance for selecting the optimal collocation window for sounding calibration and validation in weather monitoring.

The second issue is related to radiosonde data quality. RAOBs are known to suffer from radiation errors in temperature data and have various biases in humidity measurements, particularly in the upper troposphere and above. Moreover, biases in RAOBs are sonde type dependent. Currently there are dozens of sonde types flown in the global radiosonde network. This situation poses a challenge for an accurate validation of satellite soundings at local, regional, and global scales. The second purpose of this analysis is to identify differences among sonde types with a hope to bring them into relative agreement for their better use in satellite sounding performance evaluation.

A dataset of collocations of RAOBs with global positioning system (GPS) radio occultation (RO) soundings from the mission of Constellation Observing System for Meteorology, Ionosphere, and Climate (COSMIC) provided by University Corporation for Atmospheric Research (Anthes et al. 2008) is used for this study. This collocation dataset is generated from the NOAA Products Validation System (NPROVS). An introduction to NPROVS and RAOB-COSMIC collocation data is given in Section 2. Currently, NPROVS includes collocations of RAOB with fifteen different satellite sounding products and the reason COSMIC data are used for the analysis is also presented in Section 2. Methodologies of how to assess the collocation mismatch impact and identify sonde type characteristics are described in Section 3. Section 4 presents results of the impact of collocation mismatch including the radiosonde drift on satellite sounding validation. The impact is assessed separately for distance and time mismatch through understanding how the validation error varies with collocation mismatch. Radiosonde humidity observations at most stations are limited to below 200 hPa but temperature profiles generally extend to the mid-stratosphere around which balloon drift reaches a maximum distance. To gain the knowledge of the full range of mismatch, particularly the distance mismatch impact, the analysis is focused on the temperature profile validation. In Section 5, characteristics for eleven major sonde types are presented through comparing their observations with collocated COSMIC data of atmospheric temperature and refractivity with the emphasis on atmospheric humidity which has been regarded as a great uncertainty in contemporary climate monitoring application. Summary and discussions are given in Section 6.

* *Corresponding author address:* Bomin Sun, IMSG, 4231 Suitland Road, Suitland, MD 20746; e-mail: Bomin.Sun@noaa.gov.

2. RAOB-COSMIC COLLOCATION DATASET

The RAOB-COSMIC collocation dataset of April-October 2008 generated through NPROVS is used in the analysis. It consists of 77,000 pairs of collocations distributed over the globe with over 55% over the Northern hemisphere mid-latitude land areas where most of the RAOBS are concentrated.

2.1 NPROVS

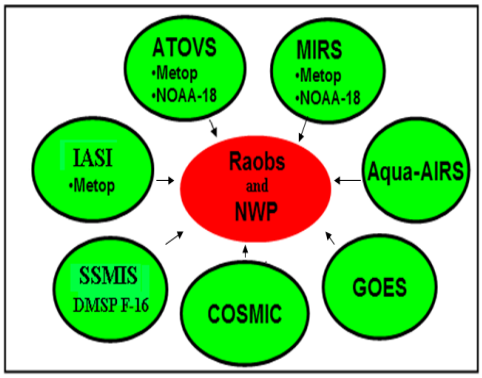

Figure 1. Schematic diagram of satellite (green) and ground truth data (Red) platforms currently accessed and collocated within NPROVS. The satellite sounding product systems are the ones generated from observations of Advanced TIROS Operational Vertical Sounder (ATOVS) from NOAA-18 and MetOp, Microwave Integrated Retrieval System (MIRS) from NOAA-18, MetOp, and Defense Meteorological Satellite Program (DMSP), Geostationary Operational Environmental Satellite (GOES), Atmospheric InfraRed Sounder (AIRS) from NASA-Earth Orbiting Satellite (EOS) Aqua, Infrared Atmospheric Sounding Interferometer (IASI) from MetOp, and Constellation Observing System for Meteorology, Ionosphere, and Climate (COSMIC) provided by University Corporation for Atmospheric Research (UCAR).

NPROVS, operated by the Office of SaTellite Applications and Research (STAR) at NESDIS provides routine compilation of collocated radiosonde and derived satellite sounding products from a constellation of five environmental satellites and ten independently operated product systems (Figure 1). The work is in support of National Polar-orbiting Operational Environmental Satellite System (NPOESS) calibration and validation of the Cross-track Infrared Sounder (CrIs) – Advanced Technology Microwave Sounder (ATMS) Environmental Data Records (EDR). More information about NPROVS including its system interface and general scientific applications can be found in Pettey et al. (2009) and Reale et al. (2009), respectively.

In NPROVS, RAOBs are treated as the "anchor" in their collocations with satellite soundings. The distance and time window for collocating COSMIC soundings to RAOBS are 250 km and 7 hr, respectively. If a COSMIC sounding falls within this window, it is picked to match with the RAOB. If multiple COSMIC soundings are within the window, only the one that is closest in distance and time to the RAOB is collocated.

2.2 Radiosonde and COSMIC Data

Radiosonde data used in NPROVS are those routinely utilized during the NOAA/Environmental Modeling Center (EMC) operational Numerical Weather Prediction (NWP) assimilation. Observational quality control markers determined during the NWP assimilation, observational corrections (i.e., due to the sensor radiative heating and cooling during flight), and ancillary information, such as balloon drift and collocated NWP data, are affiliated with the radiosonde data. Prior to NPROVS collocation, a series of quality assurance procedures have been applied to remove data records with quality problems including climatological outliers and vertical or temporal inconsistency. Profiles with vertical gaps greater than 5 km are not used for collocation. COSMIC soundings with bad quality flags are also excluded for collocation.

The COSMIC observing system consists of six satellites, each equipped with a GPS receiver. By measuring the phase delay of radio wave transmitted by GPS satellites as they are occulted by the Earth's atmosphere, the COSMIC system provides vertical profiles of atmosphere structure. Launched in April 2006, COSMIC currently yields over 2000 all-weather soundings per day distributed relatively uniformly around the globe. Vertical profiles of COSMIC refractivity (N) soundings are inverted from GPS RO bending angles, and COSMIC temperature and water vapor soundings provided by UCAR are retrieved in a near-real-time mode using the COSMIC N profiles in conjunction with a one-dimensional variational scheme that uses NCEP NWP analyses as its first-guess.

In the past, attempts were made to understand issues discussed in the Introduction by using collocations of RAOBs with polar satellites, but the relatively low horizontal and vertical resolution of the satellite data and lack of synchronization between the sun-synchronous satellite and synoptic radiosonde observations posed serious limitations (McMillin et al. 1998, Reale et al. 2008). The relatively high vertical resolution (i.e., 100 m in the low-mid troposphere and 1 km above the tropopause) and comparatively random temporal distribution of the global COSMIC observations offer a unique opportunity for understanding the collocation mismatch impact on satellite validation.

COSMIC soundings are expected to be accurate in the upper troposphere and stratosphere, and be subject to measurement errors and/or NCEP NWP model bias in the lower troposphere. Overall, the biases in the COSMIC sounding data are anticipated to be relatively small and vary smoothly in space, making comparison of different sonde types meaningful.

The parameters to be evaluated in this analysis include T, relative humidity (RH), and N. Radiosondes

directly measure T and RH. Profiles of Radiosonde N is calculated by

$$N = 77.6\frac{P}{T} + 3.73x10^5\frac{P_w}{T^2} \qquad (1)$$

where P is atmospheric pressure and P_w atmospheric vapor pressure.

For all of the analyses throughout the paper, both RAOB and COSMIC soundings are interpolated to profiles with a common 40-level pressure ranging from surface to the top of the stratosphere.

3. METHODOLOGIES

Mean difference (MEANdiff), standard deviation (STDdiff), or root mean square difference (RMSdiff) between RAOB and satellite data are the variables commonly used for evaluating satellite sounding performance in weather monitoring. In this study, these variables are calculated using the following formulas:

$$\text{MEANdiff} = \sum_{i=1}^{i=N}(X_i^r - X_i^c)\Big/N \qquad (2.1)$$

$$\text{STDdiff} = \sqrt{\sum_{i=1}^{i=N}(X_i^r - X_i^c - \text{MEANdiff})^2\Big/N} \qquad (2.3)$$

$$\text{RMSdiff} = \sqrt{\sum_{i=1}^{i=N}(X_i^r - X_i^c)^2\Big/N} \qquad (2.2)$$

Where X^r and X^c represent the values of RAOB and COSMIC parameters, respectively, the subscript i the ith RAOB-COSMIC collocation and N the total number of collocations, its value varying with the size of collocation window specified or the type of sonde flown in the global network. In addition to the intra-variability among sonde types (shown in Section 5) which is considered to remain constant with collocation mismatch, STDdiff reflects primarily the weather-scale noise introduced by the collocation distance and time mismatch. Besides the information contained in STDdiff, RMSdiff also includes the RAOB-minus-COSMIC MEANdiff, which is primarily due to the systematic difference in the way these two types of data are made.

The impact of collocation mismatch on satellite sounding validation is assessed by quantifying the change of RMSdiff with distance and time mismatch, as expressed in Equation (3.1) and (3.2), respectively.

$$\text{RMSdiff}(d) = C(d=0) + \frac{\partial(\text{RMSdiff})}{\partial(d)} x\Delta d \qquad (3.1)$$

$$\text{RMSdiff}(t) = C(t=0) + \frac{\partial(\text{RMSdiff})}{\partial(t)} x\Delta t \qquad (3.2)$$

Where C(d=0) denotes the value of RMSdiff associated with the zero value of distance mismatch, C(t=0) the zero value of time mismatch, and the partial derivative terms the sensitivity of the RMSdiff to collocation mismatch. As presented in Section 4.2, the sensitivity to distance mismatch is determined by the regression slope of the RMSdiff vs. distance mismatch for discrete time mismatch intervals (e.g., every 1 hour) and the sensitivity to time mismatch is determined by the slope of the RMSdiff *vs.* time mismatch for discrete distance mismatch intervals (e.g., every 50 km).

Characteristics of eleven sonde types which use different humidity sensors are identified by comparing their measurements with the collocated COSMIC data (see Section 5). MEANdiff *and* STDdiff for each of the sonde types are calculated using Equations (2.1) and (2.2), respectively, and N in this case is the number of collocations of the sonde type with the COSMIC over the globe. If the sonde type characteristics through analyzing MEANdiff and STDdiff are consistent with known biases and/or published findings (e.g., from laboratory and field experiments or other observations), we tend to think the differences or biases of sonde types (relative to COSMIC) are most probably true and COSMIC data are able to distinguish differences among sonde types. In this analysis, to corroborate the sonde type characteristics identified using COSMIC data, polar satellite observations are compared with radiances calculated from collocated RAOBs using the Community Radiative Transfer Model (CRTM, Han et al. 2006, see Section 5).

All of the computation results of interest in this study are tested for statistical significance.

4. COLLOCATION MISMATCH IMPACT

4.1 Drift Impact Assessment

The conventional way to calculate the RAOB-satellite collocation mismatch is based on the balloon launch site location and release time, and the location of satellite sounding footprint on the Earth's surface and its overpass time.

Different from polar or geostationary satellite soundings, COSMIC occultation soundings also drift. Generally the occultation trajectory drifts horizontally 150 km and takes about 2 min when it descends from 60 km height to the surface. The 2-min time is believed not to cause any difference in the mismatch impact estimation and the time value at the COSMIC "occultation point" is therefore assigned to all levels of COSMIC soundings. COSMIC "occultation point", generally located 2-4 km above the surface along the occultation trajectory, is meant to be representative of the whole COSMIC sounding profile. The RAOB-COSMIC collocation mismatch is defined below for *drift-not-considered* and *drift-considered* cases, respectively.

- *Drift-not-considered*: the mismatch is calculated based on the radiosonde balloon launch site location and release time, and the location and time of the COSMIC "occultation point";

- *Drift-considered*: the mismatch is calculated for each level of the 40-level profiles, based on the balloon drift location and time, and the same-level's COSMIC sounding location and the "occultation point" time.

Two methods are available to select collocation samples for the *drift-considered* case. Method 1 selects *only* the whole profiles of radiosonde and collocated COSMIC, which requires their mismatches from surface to the top of the profiles be all within the specified mismatch window; for Method 2, only levels for which the mismatches are within the specified window are used. Collocation samples from Method 1 are generally much less than Method 2 but the drift impact results are found to be similar between them (not shown). The drift impact is estimated by comparing the *drift-not-considered* RMSdiff with the *drift-considered* one.

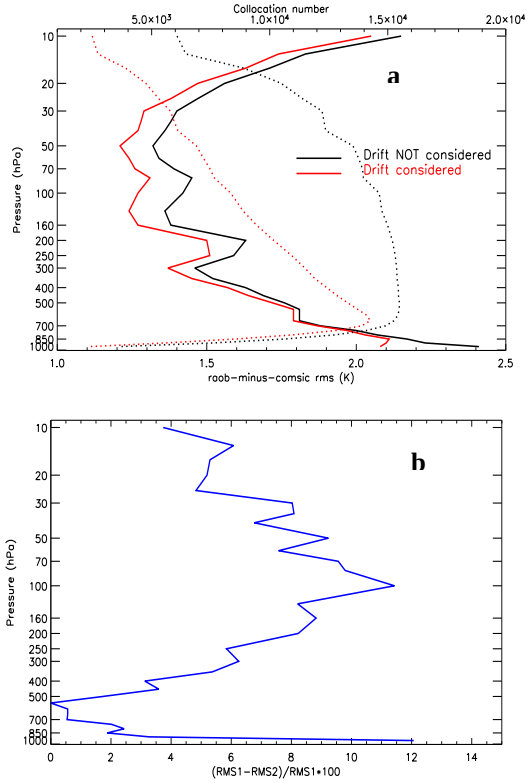

Figure 2. (a) RAOB-minus-COSMIC temperature RMSdiff for *drift-not-considered* (black solid) and *drift-considered* (red solid), respectively. Their sample sizes are denoted as the black and red dotted curves, respectively. (b) Percentage difference of the RMSdiff between these two cases. F-test indicates that except the levels between 750 hPa and 550 hPa, the drift impact on the RMSdiff is statistically significant at the 0.05 or better levels.

Figure 2 shows the drift impact on the temperature RMSdiff. Data of RAOB-COSMIC collocations within the distance mismatch of 150 km and time mismatch of 4 hr are used for the calculation, and samples for the *drift-considered* case are picked using Method 1 described at the above paragraph. As seen in Figure 2, the *drift-considered* RMSdiff is smaller than for *drift-not-considered,* particularly in the tropopause and lower stratosphere, where the difference is reduced by 8-10% when the drift is taken into account. The small difference in the RMSdiff between these two cases over the low-to-mid troposphere (750-550 hPa) is because the drifts in both distance and time are small. COSMIC soundings can not penetrate into near-surface levels of the atmosphere particularly in the moist environment, causing the number of RAOB-COSMIC collocation samples too low (Figure 2a) which biases the drift impact analysis for those levels.

4.2 Sensitivity of the RAOB-mInus-COSMIC RMS Difference to Collocation Mismatch

The drift impact revealed in Section 4.1 has been taken into account for the analysis presented in this sub-section by using Method 2 (described in Section 4.1) to select the RAOB-COSMIC collocation samples for individual levels of the profiles.

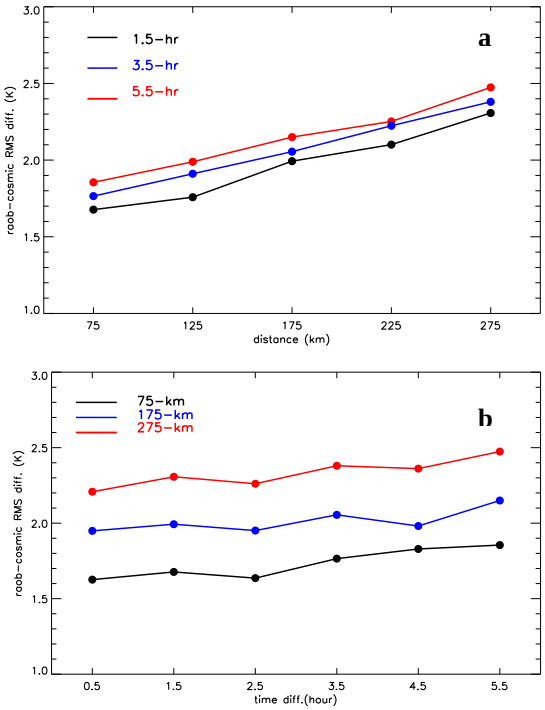

Figure 3. Changes of the 500 hPa temperature RMSdiff with distance mismatch (a) and time mismatch (b). Black, blue and red curves denote the RMSdiffs calculated from collocations with time mismatch of around 1.5 hr, 3.0 hr, and 5.5 hr, respectively (a), and with distance mismatch of around 75 km, 175 km, and 275 km, respectively.

Figure 3 shows an example of how the sensitivity of RMSdiff to collocation mismatch is assessed. The RMSdiff increases with the increase in distance

mismatch (Figure 3a) and the regression slopes for the time mismatch of 1.5 hr, 3.5 hr, and 5.5 hr are 0.31 K/100 km, 0.30 K/100 km, and 0.27 K/100 km, respectively. All these values are found to be statistically significant at the 0.05 or better levels. Correspondingly, the regression intercept values are 1.43 K, 1.53 K, 1.66 K, respectively, suggesting the weather-scale noise introduced due only to time mismatch increases with it. Similarly, the RMSdiff also increases with time mismatch for the distance mismatch of 75 km, 125 km, and 225 km, respectively (Figure 3b). The regression slopes for these three cases are 0.15 K/3 hr, 0.09 K/3 hr, and 0.14 K/3 hr, respectively, which are statistically marginally significant. Their regression intercept values are 1.58 K, 1.92 K, and 2.19 K, increasing with distance mismatch from 75 km to 125 km, and to 225 km.

Similar analysis was done for all other levels. Vertical profiles of the regression intercept and slope values for distance and time mismatch are depicted in Figure 4 and 5, respectively.

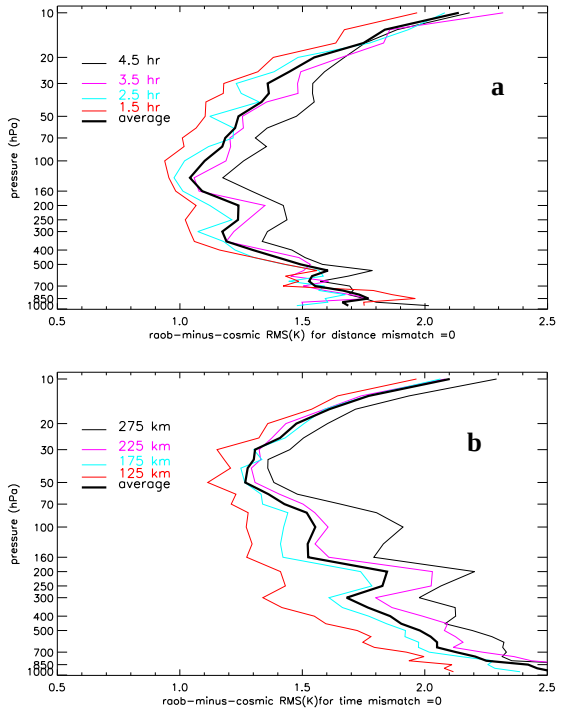

Figure 4. Temperature RMSdiff associated with the zero value of distance mismatch (a) and time mismatch (b) calculated from the linear regression analysis (see text). Thin curves in (a) and (b) indicate the RMSdiffs are calculated from collocations with different time and distance mismatches, respectively. Thick black curves in both plots denote the values averaged from the thin curves.

The RMSdiff associated with the zero value of distance mismatch and 1.5-4.5 hr of time mismatch decreases with a value of 1.6 K at the lower troposphere to 1.0 K around the tropopause and then increases to 2.0 K at the mid-stratosphere (Figure 4a), and the RMSdiff associated with the zero value of time mismatch and 125-275 km of distance mismatch decreases with a value of 2.3 K at the lower troposphere to 1.4 K at the lower stratosphere and then increases to 2.0 K at the mid-stratosphere (Figure 4b). As stated in Section 3, these intercept values contain the sonde type intra-variability, the RAOB-minus-COSMIC systematic difference, and the collocation mismatch induced weather noise. It would be interesting to see how the RMSdiff profiles in Figure 4 change when both the distance and time mismatch values are close to zero. This will be investigated in the future when enough collocation samples are accumulated. Figure 4 also indicates for all the levels from surface to 10 hPa RMSdiff increases with the increase in time mismatch (Figure 4a) and distance mismatch (Figure 4b), respectively. This is consistent with the findings from the RMSdiff sensitivity analysis shown in Figure 5.

The distance sensitivity becomes smaller from surface to the lower troposphere and then gradually increases and reaches a maximum around the tropopause and then it becomes smaller and goes near zero when the height goes towards the lower and middle stratosphere (Figure 5a). At the upper troposphere and tropopause where jet streams are located, horizontal gradients of temperature are much greater than at other heights. This may explain why the maximum sensitivity occurs around there. The sensitivities are found to be statistically significantly at the 0.05 or better levels for heights below 50 hPa. Overall, the RMSdiff sensitivity to distance mismatch is ~0.35 K/100 km for the troposphere and 0.05-0.20 K/100 km for the low-to-mid stratosphere.

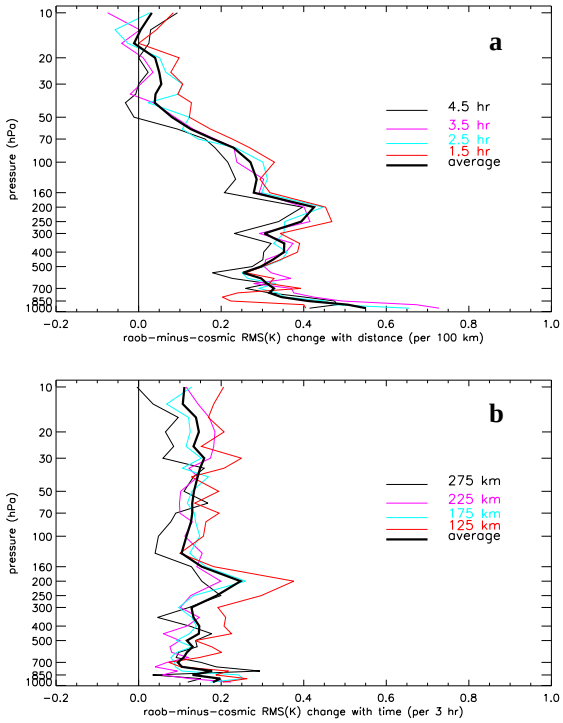

Figure 5. Temperature RMSdiff sensitivity to collocation distance mismatch (a) and time mismatch (b). As in Figure 4, thin curves in both plots are calculated using collocations with different mismatch values, and thick black curves are the averages of the thin curves. Sensitivity to distance mismatch is represented as the RMSdiff in Kelvin per 100 km (a) and to time mismatch is represented as the RMSdiff in Kelvin per 3 hr.

The RMSdiff sensitivity to time mismatch (Figure 5b) shows vertical changes basically similar to the distance mismatch for the troposphere, but the sensitivity to time mismatch remains stable throughout the stratosphere. The sensitivities are statistically significant at the 0.05 or better levels for heights above 400 hPa. Overall, the sensitivity to time mismatch is ~0.20 K/3 hr.

To summarize, the RAOB-COSMIC temperature RMSdiff is impacted by both the collocation distance and time mismatch. Based on the linear regression analysis, the RMSdiff associated with the zero value of distance mismatch and 1.5-4.5 hr of time mismatch reaches 1.6 K at the lower troposphere and reduces to 1.1 K in the upper troposphere, and these numbers are expected to increase with distance mismatch by ~0.35 K/100 km; the RMSdiff associated with the zero value of time mismatch and 125-275 km of distance mismatch reaches 2.3 K at the lower troposphere and reduces to 1.5 K in the upper troposphere, and these numbers are expected to increase with time mismatch by ~0.20 K/3 hr. Radiosonde drift increases the RAOB-satellite collocation mismatch and the analysis of RAOB-COSMIC collocation data indicates taking into account of the drift of both RAOB and COSMIC soundings reduces their temperature RMSdiff by ~10% around the tropopause and lower stratosphere where the jet streams are located.

5. IDENTIFYING SONDE TYPE CHARACTERISTICS

Type	BUFR code	Manufacturer or Country	T sensor	RH sensor	report
RS80	**037, 060, 061, 062, 063, 052, 067**	**Vaisala (Finland)**	**Bead thermocap**	**A/H Humicap**	**1038**
RS90	**071**	**Vaisala (Finland)**	**Thin wire F-thermocap**	**Twin H Humicap**	**873**
RS92	**079, 080, 081, 034**	**Vaisala (Finland)**	**Thin Wire F-Thermocap**	**Twin H-Humicap**	**5862**
M2K2 & M2K2-DC	**057,056**	**Modem (France)**	**Bead or chip thermistor**	**Capacitive polymer**	**333**
DFM-90 & DFM-06	**050, 017**	**Graw (Germany)**	**Bead thermistor**	**Capacitive polymer**	**89**
RS2-91 & RS-01G	**047, 055**	**Meisei (Japan)**	**Rod thermistor**	**Capacitive polymer**	**317**
VIZ & Sippican	**049, 051, 084, 086, 085, 087**	**VIZ, Sippican (U.S.)**	**Rod or Chip thermistor**	**Carbon hygristor**	**2245**
Mark IV	**020**	**IMD (India)**	**Rod thermistor**	**Carbon hygristor**	**85**
Shang-E	**032**	**Shang (China)**	**Rod thermistor**	**Carbon hygristor**	**452**
VIZ/Jing Mark II	**021**	**Jinyang (Korea)**	**Rod thermistor**	**Carbon hygristor**	**81**
MRZ, MARS, RKZ, etc	**028, 029, 027, 075, 088, 058, 089, 068, 069**	**AVK (Russia)**	**Rod thermistor**	**Goldbeater's skin hygrometer**	**3585**

Table 1: Major sonde types used in this study. RAOB reports are counted from data of April to October 2008 of the operational global radiosonde network.

As listed in Column 2 of Table 1, most of the eleven sonde types have several sub-types indicated by the 3-digit sonde instrument bufr codes. The eleven sonde types can be grouped into three big types following the humidity sensors they use: capacitive polymers in Finnish Vaisala RS80, RS90, and RS92, French Modem, Germany Graw, and Japanese Meisei; carbon hygristor in U.S. VIZ & Sippican Mark, Indian Mark IV, Chinese Shang-E, and South Korean VIZ/Jinyang; and Goldbeater's skin sensor in Russian sondes. Capacitive polymer and carbon hygristor sensors have been found to show dry biases particularly in the upper troposphere due mainly to the slow or no response to the humidity change when the atmosphere is cold, and Goldbeater' skin sensor has been known to have a moist bias throughout the troposphere (Wang and Zhang, 2008). Although the sonde types within any of these three groups are subject to the same general sources of RH measurement bias, the magnitude or even the sign of the bias depends critically on the specific sonde type and the way its observations are made, as will be shown in this section.

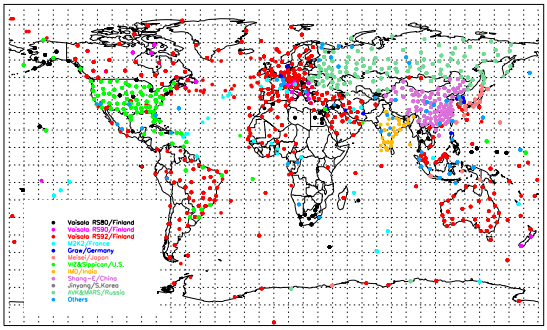

Figure 6. Spatial distribution of major radiosonde types (listed in Table 1) flown in the existing global network.

Most of the dots on the map (Figure 6) represent stations with a specific sonde type flown but multiple sonde types are found in the reports of the same

stations for some stations in Russia and a few stations in other areas. RS92 (red dot) is the most widely used sonde type, flown over many parts of the world, including Australia, South America, Europe, Canada, West Africa, and many islands of the global oceans. VIZ-B2, RS80 and particularly Sippican Mark IIA are the major sonde types flown in the U.S. network. Starting January 2002 the digital Shang-E with a carbon hygristor was introduced into the Chinese network with a total number of 90 stations, replacing Shang-M with Goldbeater's skin, and up to August 2008, Shange-E has been used in 82 stations. Over ten sonde types are flown in the Russian upper air network and nine of them with the rod thermistor and Goldbeater's skin are picked for the analysis.

The RAOB-minus-COSMIC MEANdiff and STDdiff of different sonde types are shown in Figures 7.1, 7.2, and 7.3 for RH, T, and N, respectively. These figures are intended to give the reader a general idea of measuring behavior (relative to COSMIC) of those sonde types (relative to the COSMIC data). More detailed discussion of their characteristics is presented later in this section.

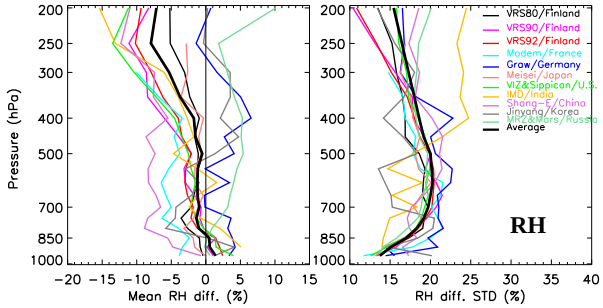

Figure 7.1. Raob-minus-COSMIC relative humidity RMSdiff (left) and STDdiff (right) for different sonde types listed in table 1. Values of thick black curves are calculated using samples of all of the sonde types.

Relative to COSMIC, most of the sonde types show a dry bias particularly in the upper troposphere (left plot of Figure 7.1). This is consistent with Soden and Lanzante (1996) who compared radiosonde data with satellite measurements and Wang and Zhang (2008) who compared radiosonde data with ground-based GPS total precipitable water data. The moist bias throughout the troposphere in Russian Goldbeater's skin sensor is also noticed in these two studies.

Anomalous STDdiffs (right plot of Figure 7.1) are seen in Germany Graw, South Korean VIZ/Jinyang, and Indian Mark IV. The poor performance of these sonde types also appears in T (Figure 7.2). It is suspected that India has been testing several new varieties of IMD Mark IV and is using the new and old sondes interchangeably at many stations, and some of the dates for these transitions are probably inaccurate (Schroder 2009). So the degree of dry or moist bias can vary erratically at the same station and should differ between stations. Similar situations are also suspected to occur to Germany Graw and South Korean VIZ/Jinyang, both of which otherwise would have a dry bias based on the characteristics of instruments (Table 1) specified in their respective RAOB reports.

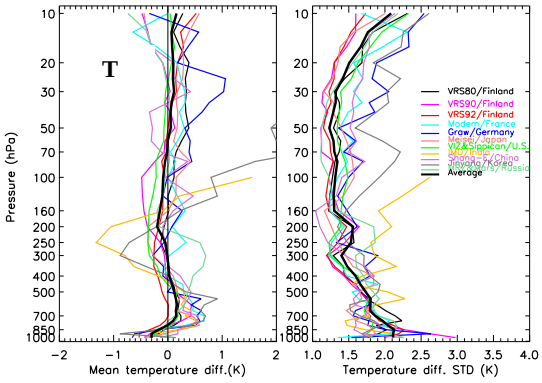

Figure 7.2. Same as Figure 7.1 except for atmospheric temperature.

For most of the sonde types with the exception of Indian, South Korean, and Germany ones, temperature observations are close to the COSMIC (Figure 7.2). On average, the difference between RAOB and COSMIC is within 0.1-0.2 K at the levels above 500 Hpa. The negative and positive MEANdiff (left plot of Figure 7.2) at the near-surface and low troposphere shown in most of the sonde types are perhaps related to the ambiguous parsing of COSMIC T from N.

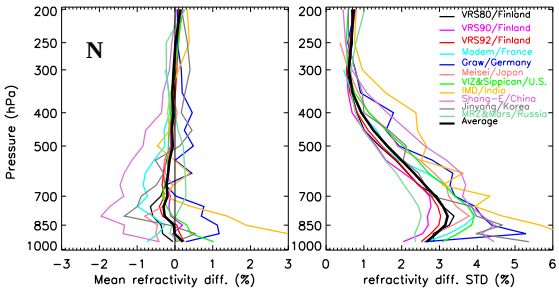

Figure 7.3. Same as Figure 7.1 except for atmospheric refractivity.

Atmospheric refractivity is sensitive to temperature in the upper troposphere and humidity in the lower troposphere. As expected from their poor performance in T and RH, refractivity for Indian, South Korean, and Germany sondes are among the worst. Due to its great dry bias throughout the troposphere, refractivity for the Chinese sonde is also among the worst (Figure 9). Refractivity for RS90 and RS92 is among the best despite their great dry biases in the upper troposphere (Figure 8).

Vaisala RS type and U.S. VIZ & Sippican are among the sonde types whose characteristics have been relatively well documented. Are the characteristics of these sonde types identified using the COSMIC consistent with the ones in literature?

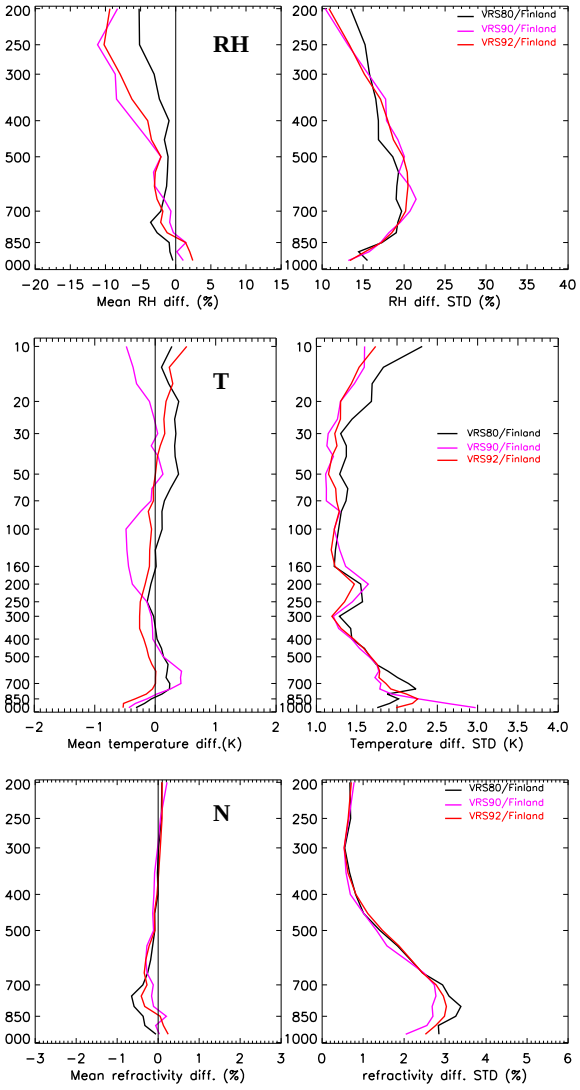

Figure 8. Intercomparison of RS80, RS90, and RS92 for RH (top), T (middle), and N (bottom).

As seen in Figure 8, both RS90 and RS92 show a similar dry bias (e.g., of 10% at 250-300 hPa) and STDdiff throughout the troposphere. This similarity is consistent with the fact that they are essentially equivalent sensors in terms of calibration accuracy and time response (Miloshevich et al. 2006). The dry bias for RS90 and RS92 is found to be greater than the one in RS80, probably a result of solar radiative heating of the RS90 and RS92 twin H-Humicap sensor both prior to launch and during flight while an aluminized plastic shield is installed over the RS80 A/H Humicap (Wang and Zhang 2008).

The RS92 temperature sensor with a fast response time and small radiation correction in all weather conditions, is considered to be one of the best sensors (Miloshevich et al. 2006). Both RS90 and RS92 are far better than the RS80 (Figure 8), which has an error in the radiation correction (on RS80-57H) that has been documented (Redder et al. 2004).

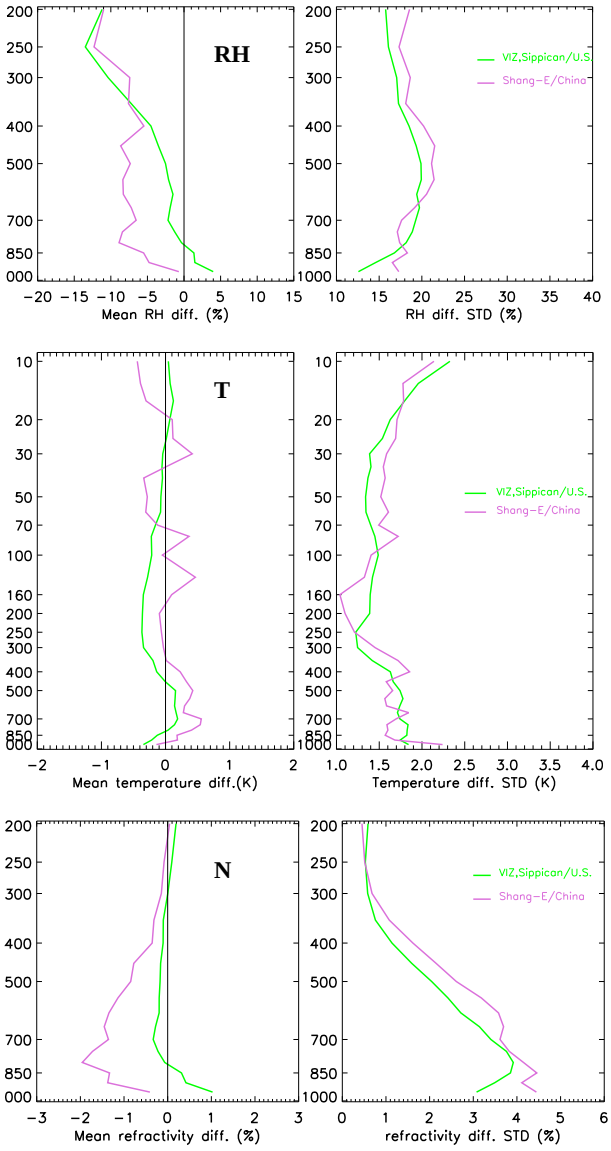

Figure 9. Same as Figure 8 except for the U.S. VIZ & Sippican and Chinese Shang-E.

A dry bias is shown in the U.S. Sippican & VIZ carbon hygristor from 700 hPa to the upper troposphere where the bias reaches 10-15% (Figure 9). This is consistent with what has been found about Sippican & VIZ carbon hygristors: time-lag error throughout the troposphere and failure to respond to humidity changes in the upper troposphere, sometimes in the middle

troposphere when the temperature is colder than -34C (Wang et al. 2003).

In addition to a dry bias of 10-15% at the upper troposphere, the Chinese Shang-E carbon hygristor shows a dry bias of ~10% consistently from 850 hPa to 300 Hpa. This may be related to the fact the Shang-E carbon hygristor was calibrated against RS80-A which was about 5-15% drier than that of the dew point hygrometer, but the Shang-E dry bias in the low-to-mid troposphere appears to be greater than the one in RS80-A.

The negative refractivity bias in Shang-E is caused predominately by the dry bias as its temperature is close to the COSMIC. Besides the dry bias, the slight cold bias in the mid-troposphere to lower stratosphere in VIZ & Sippican sondes adds a negative bias to their refractivity for these heights.

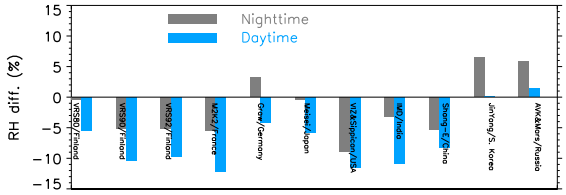

Figure 10. Raob-minus-COSMIC relative humidity MEANdiff at 300 Hpa for different sonde types (listed in Table 1) for daytime and nighttime .

The sonde type evaluation described this section above was based on the data with daytime and nighttime observations mixed. Figure 11 indicates that for all of the sonde types the upper air RH bias in daytime is greater than the nighttime. This is consistent with the fact that humidity sensors tend to have a dry bias from the solar radiative heating. Statistically significant day *vs.* night differences (at the 0.05 or better levels) are found for RS80, RS90, RS92, Modem, Graw, VIZ/Jinyang and Goldbeater. On average, the day *vs.* night MEANdiff is -7.1% *vs.* -2.8%, which is significantly different to each other at the 0.001 level.

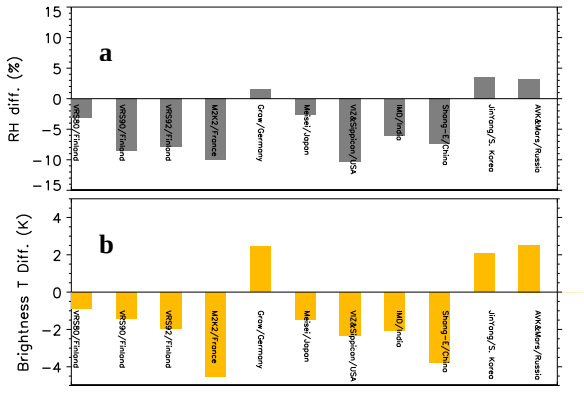

Figure 11. Relative humidity MEANdiff (relative to COSMIC) at 300 hPa (a) and brightness temperature difference (relative to Microwave Humidity Sensor upper tropospheric channel 3 observations) (b).

To gain more confidence in the ability of COSMIC to identify sonde type characteristics, they are cross-checked by using independent satellite observations. Figure 11a shows the sonde type 300hPa RH bias relative to the COSMIC. The difference between upper-air humidity-sensitive brightness temperature (BT) calculated from sonde type temperature and water vapor profiles using CRTM and the collocated observed Microwave Humidity Sensor (MHS) channel 3 BT is shown in Figure 11b. The BT biases in Figure 11b can be converted to RH biases using the regression analysis technique (Soden and Lanzante 1998), and the qualitative agreement between these two biases, nevertheless, indicates the sonde type biases identified by COSMIC are probably true, at least in sign.

To summarize, MEANdiff and STDdiff (see Equation 2) for eleven sonde types of interest calculated from global RAOB-COSMIC collocation data were analyzed for RH, T and N. The sonde type characteristics identified this way are basically consistent with what have been found through field experiments and comparing with other data, indicating COSMIC data probably can be used as a candidate to bring different sonde types into relative agreement for their better use in satellite sounding validation.

6. SUMMARY AND DISCUSSION

Based on seven months of NPROVS RAOB-COSMIC collocation data, this work analyzed the impact of RAOB-COSMIC collocation mismatch including their drift on weather sounding validation and identified the characteristics of major sonde types flown in the existing global network.

The collocation mismatch impact was assessed by analyzing how the RAOB-minus-COSMIC RMSdiff calculated from global collocations (Equation 2.3) varied with distance and time mismatch, separately. Based on the linear regression estimation, the RMSdiff associated with the zero value of distance mismatch and 1.5-4.5 hr of time mismatch (i.e., the regression intercept) reaches 1.6 K at the lower troposphere and reduces to 1.1 K in the upper troposphere, and these numbers are expected to increase with distance mismatch by ~0.35 K/100 km (i.e., the regression slope); the RMSdiff associated with the zero value of time mismatch and 125-275 km of distance mismatch (i.e., the regression intercept) reaches 2.3 K at the lower troposphere and reduces to 1.5 K in the upper troposphere, and these numbers are expected to increase with time mismatch by ~0.20 K/3 hr (i.e., the regression slope). In addition to the collocation mismatch induced weather noise, the regression intercept RMSdiff values discussed in the analysis contain the RAOB-minus-COSMIC MEANdiff and the sonde type intra-variability.

Radiosonde drift increases the collocation mismatch and taking into account the drift of both RAOB and COSMIC soundings reduces their temperature RMSdiff by ~10% around the tropopause and lower stratosphere where the jet streams are located. This analysis indicates that the performance of satellite soundings, when evaluated by collocated RAOBs or other ground-truth data, is expected to become better with the size of collocation window (used to pick the collocation samples) becoming smaller, given the availability of data with satisfying spatial and temporal representative.

As emphasized throughout this work, the RMSdiff or STDdiff defined in Equation 2 is impacted primarily by weather-scale noise introduced by the distance and time mismatch between radiosonde launch and satellite overpass. Does the mismatch also impact the detection of long-term climate trend using satellite observations if calibrated by collocated radiosonde or other "ground-truth" data? Trend detection could be impacted if the RAOB-minus-satellite mean difference and/or standard deviation calculated using monthly data (as opposed to the synoptic data expressed in Equation 2) increases significantly with the increase in distance and time mismatch. This, if true, could impact the sampling strategies and principles under development for the proposed upper air climate reference network (WMO 2008).

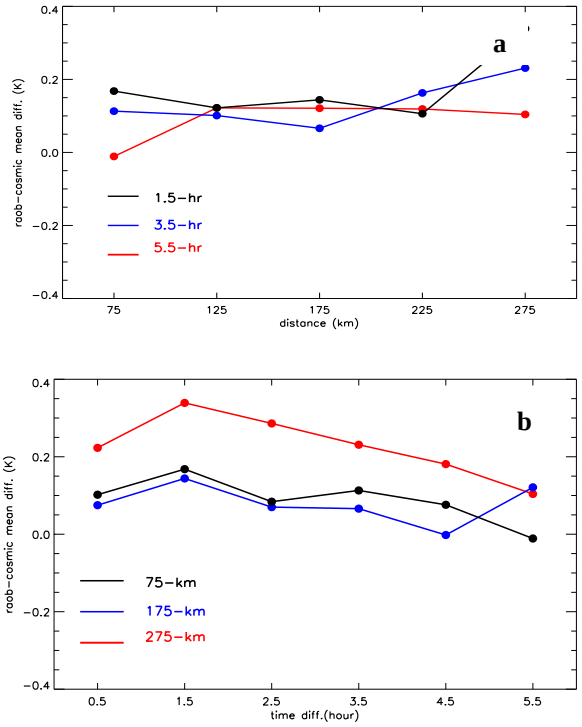

Figure 12. Same as Figure 3 except for Raob-minus-COSMIC temperature MEANdiff.

Figure 12 indicates that the collocation mismatch does not appear to cause a significant impact on the RAOB-minus-satellite mean difference which in this case is averaged from seven months of data. The short collocation data record available at this time prevents us from evaluating the mismatch impact on the standard deviation of the monthly RAOB-minus-satellite difference, but it is in our plan to do so once enough length of data are accumulated.

Characteristics of eleven major sonde types were identified by analyzing the RAOB-COSMIC MEANdiff and STDdiff (see Equation 2) calculated from the global data. The following results were among those found from the analysis.

- Most of the sonde types show a dry bias particularly in the upper troposphere where the bias reaches ~10% in RH.
- Daytime RH biases for all of the sonde types tend to be drier than the nighttime (e.g., by 4.3% at 300 hPa on average).
- RS90 and RS92 show a dry bias similar to each other but greater than the one in RS80, perhaps a result of solar radiative heating on the RS90 and RS92 humidity sensor; a warm bias is shown in the RS80 temperature data, resulting perhaps from an incorrect radiation correction.
- Temperatures for most of the sonde types are found to be within 0.1-0.2 K of the COSMIC data throughout the atmospheric column.
- RS92 is among the best among the sonde types in terms of refractivity accuracy despite its dry bias of ~10% in the upper troposphere.
- Poor performance of T, RH and N data was found in the Indian, South Korean and Germany sondes, related perhaps to inaccurate reporting information specified in the data and/or abnormal way the reports were made.
- Chinese Shang-E is among the worst in terms of refractivity accuracy, due to the 10-15% dry bias in its carbon hygristor measurements throughout the lower to upper troposphere.

The measuring characteristics revealed in this study for different sonde types are basically consistent with what have been documented in literature. The 300-hPa humidity biases in sonde types (relative to the COSMIC data) are also consistent with their comparison with collocated satellite MHS upper-peaking brightness temperature observations. All these appear to indicate the biases in sonde types identified in the analysis are likely to be real and are recommended to be considered when RAOBS are used to validate and calibrate satellite sounding retrievals.

Considered that only seven months of data used, results shown in this study are preliminary and the topics will be re-visited when more data are accumulated. This study, nevertheless, demonstrates

the usefulness of NPROVS in satellite validation/calibration, and weather and climate monitoring.

6. REFERENCES

Anthes, R.A., and Coauthers, 2008: The COSMIC/FORMOSAT-3 Mission: Early results. *Bulletin of American Meteorological Society*, 89, 313-333.

Han, Y., F. P. van Delst, Q. Liu, F. Weng, B. Yan, R. Treadon, and J. Derber, 2006: JCSDA Community Radiative Transfer Model (CRTM) – Version 1. *NOAA Tech Report 122*.

McMillin, L.M., M.E. Gelman, A. Sanyal, and M. Sylva, 1988: A method for the use of satellite retrievals as a transfer standard to determine systematic radiosonde errors. *Monthly Weather Review*, 116, 1091-1102.

Miloshevich, L.M., H. Vömel, D.N. Whiteman, B.M. Lesht, F.J. Schmidlin, and F. Russo, 2006: Absolute accuracy of water vapor measurements from six operational radioosnde types launched during AWEX-G and implications for AIRS validation. *Journal of Geophysical Research*, 111, D09S10, doi:10.1029/2005JD006083.

Pettey, M., B. Sun and A. Reale, 2009: The NOAA product (integrated) validation system (NPROVS) and environmental data graphical evaluation (EDGE) interface part-2: system. *25th Conference on International Interactive Information and Processing Systems (IIPS) for Meteorology, Oceanography and Hydrology,* 89th AMS Annual Meeting, Phoenix, AZ, 11-15 January.

Reale, A., F. Tilley, M. Ferguson, and A. Allegrino, 2008: NOAA operational sounding products for ATOVS, *International Journal of Remote Sensing*, 29, 4615-4651.

Reale, A., B. Sun and M.Pettey, 2009: The NOAA product (integrated) validation system (NPROVS) and environmental data graphical evaluation (EDGE) interface part-1: science. *5th Annual Symposium on Future Operational Environmental Satellite Systems-NPOESS and GOES-R,* 89th AMS Annual Meeting, Phoenix, AZ, 11-15 January.

Redder, C., J. Luers, and R. Eskridge, 2004: Unexplained discontinuity in the U.S. radioosnde temperature data. Part II: Stratosphere. *Journal of Atmospheric and Oceanic Technology*, 21, 1133-1144.

Schroeder, S.R., 2009: Validating and completing global historical radiosonde metadata by examination of sensitive variables. *Journal of Climate* (submitted).

Soden, B.J., and J.R. Lanzante, 1996: An assessment of satellite and radiosonde climatologies of upper-tropospheric water vapor. *Journal of Climate*, 9, 1235-1250.

Wang, J., and L. Zhang, 2008: Systematic errors in global radiosonde precipitable water data from comparisons with ground-based GPS measurements. *Journal of Climate*, 21, 2218-2238.

Wang, J., D.J. Carlson, D.B. Parsons, T.F. Hock, D. Lauritsen, H.L. Cole, K. Beierle, and N. Chamberlain, 2003: Performance of operational radiosonde humidity sensors in direct comparison with a chilled mirror dew-point hygristor and its climate implication. *Geophysical Research Letter*, 30, 1860, doi:10.1029/2003GL016985.

World Meteorological Organization, 2008: Report of the GCOS reference upper-air network meeting. *GCOS-121*, WMO/TD No. 1435.